UFSM

Geografia Ensino & Pesquisa

ISSN 2236-4994
OPEN ACCESS

Geog Ens Pesq, Santa Maria, v. 27, e65070, p.1-25, 2023 https://doi.org/10.5902/2236499465070
Submitted: 03/04/2021 • Approved: 09/02/2023 • Published: 17/11/2023

Geoinformation and Remote Sensing

Canopy height estimation of sugarcane varieties using an Unmanned Aerial Vehicle (UAV) and integration to satellite images

Estimativa da altura de variedades de cana-de-açúcar usando um Veículo Aéreo Não Tripulado (VANT) e integração com imagens de satélite

Gabriela Zoli Simões[I], Hermann Johann Heinrich Kux[I], Fábio Marcelo Breunig[II], Luiz Henrique Pereira[III]

[I] Instituto Nacional de Pesquisas Espaciais, São José dos Campos, SP, Brasil
[II] Universidade Federal de Santa Maria, Santa Maria, RS, Brasil
[III] IDGeo - Geointeligência Agrícola, Piracicaba, SP, Brasil

ABSTRACT

The objective of this study is to estimate the canopy height of three sugarcane varieties at different growth stages, with UAV data and to evaluate its relationship with two vegetation indices (VIs) (NDVI and EVI) at different spatial resolutions (3m, 10m and 30m). The indices were calculated using images from the PlanetScope, Sentinel-2, and Landsat 8 satellites, acquired as close as possible to the UAV imaging date. The estimated canopy height for each field was obtained by subtracting the Digital Surface Model (DSM) from the Digital Terrain Model (DTM), built by the Structure from Motion (SfM) technique with UAV RGB images as input. The average from each estimated height was compared with the average measured in the field, to verify the accuracy of the model. Both Pearson's correlation and the Determination Coefficient (R^2) were calculated between the estimated heights and the VIs. The average estimated canopy height and measurements in the field were different ($p<0.05$), with the model generally underestimating the height. However, the plantation's surface models portrayed the spatial variability within the field. The use of GCPs is mandatory to reduce errors in estimation. Regarding the indices, the spatial resolution did not influence the correlation analysis, with NDVI showing higher values than EVI, except for area A. However, all values, for both coefficients, were below 0.5 for all areas. Despite that, a temporal analysis is necessary to improve the relationship between the canopy height and VIs. The potential of UAV data as a proxy to zonal management should be addressed in future studies.

Keywords: UAV; Remote sensing; Structure from motion; Canopy height

RESUMO

O objetivo deste trabalho foi estimar a altura do dossel de três variedades de cana-de-açúcar em diferentes estágios fenológicos, utilizando dados de um VANT e avaliar sua relação com dois índices de vegetação (IVs) (NDVI e EVI) em diferentes resoluções espaciais (3m, 10m e 30m). Para o calcular os índices foram utilizadas imagens dos satélites PlanetScope, Sentinel-2 e Landsat 8, adquiridas o mais próximo possível da data do voo com o VANT. A altura estimada para cada talhão foi obtida pela subtração entre o MDS e MDT construídos a partir das imagens RGB do VANT, por meio da técnica SfM. As médias de cada altura estimada foram comparadas com médias obtidas em campo, a fim de se verificar a acurácia do modelo. Uma análise de correlação de Pearson e o coeficiente de Determinação (R^2) foram calculados entre as alturas estimadas e os IVs. As médias de altura estimada e medidas em campo foram diferentes ($p<0,05$), com o modelo, geralmente, subestimando a altura. Todavia, os modelos de superfície da plantação conseguiram retratar a variabilidade espacial do talhão. É recomendado o uso de GCPs para reduzir os erros na estimativa. Em relação aos índices, a resolução espacial não exerceu influência na análise de correlação, com NDVI apresentando valores maiores que o EVI, com exceção da área A. Contudo, todos os valores, de ambos os coeficientes ficaram abaixo de 0,5 para todas as áreas. Ainda assim, se faz necessária uma análise temporal para compreender melhor a relação entre altura e os IVs. O potencial dos dados de UAV para o gerenciamento zonal deve ser abordado em estudos futuros.

Palavras-chave: VANT; Sensoriamento remoto; Structure from motion; Altura do dossel

1 INTRODUCTION

The use of Remote Sensing (RS) techniques benefits the agriculture with the reduction of costs and environmental impacts, and increasing the productivity and profitability, as recommended by Precision Agriculture (PA). PA became possible due to the advent of technologies such as GNSS (Global Navigation Satellite System), orbital imaging, Artificial Intelligence, integration of different sensor types, sensors with automatic controls, and unmanned aerial vehicles (UAVs) (Zhang; Wang; Wang, 2002).

PA seeks to increase production efficiency, reducing the use of inputs and costs, through management practices that aim to meet the needs of each area, seeking not to consider the cultivation medium as a homogeneous region (Mulla, 2012). To reach these goals, RS is a fundamental tool, as it can provide such information in a non-destructive basis, with spatial and temporal distributed continuity, at different scales.

The main applications of RS in PA can be classified into three categories according to Hunt & Daughtry (2017): 1) the exploration of possible problems, using real-time

videos, without requiring much costs or complex analysis; 2) the monitoring to obtain advanced information, enabling actions and thus to avoid production losses; and 3) the planning of plantation management operations, which is the niche with the highest economic return, but also the one that demands more on data acquisition and analysis, presenting a higher cost than the others. Among these three classes, monitoring is still the most frequent applied category in PA practices. The main analysis performed with UAVs include the detection of water stress (Santesteban *et al*., 2017; Hoffman *et al*., 2016; Quebrajo *et al*., 2018; Bian *et al*., 2019); estimation of soil salinity (Ivushkin *et al*., 2019) and; chlorophyll concentration (Elarab *et al*., 2015); lodging (Chu *et al*., 2017; Liu *et al*., 2018); monitoring of biomass and production (Bendig *et al*., 2015, Sanches *et al*., 2018; Grüner; Astor; Wachendorf, 2019); fault detection (Luna; Lobo, 2016; Souza *et al*., 2017a), field zoning (Damian *et al*., 2017; Breunig *et al*., 2020a; Damian *et al*. 2020) and crop growth assessment (Bendig; Bolten, Bareth, 2013; Souza *et al*., 2017b).

In Brazil, one of the sectors that have taken advantage of remote sensing techniques to improve management practices and consequently increase productivity is the sugarcane sector. A proof of this, is the production increase in the 2019/20 harvest, as evidenced by CONAB (2020). According to the survey conducted, the Brazilian sugarcane production reached 642.7 million tons in the 2019/20 harvest, an increase of 3.6% in relation to the previous year. Most of this production is concentrated in São Paulo State (342.6 million tons). However, despite the increase of more than 3% in the country's production, the total planted area decreased by 1.7%, a proof that management practices focused on increase of productivity are fundamental for the development of a more sustainable agricultural production, capable of meeting market demands with the possibility of maintaining or reducing the planted area.

The main application of RS techniques in sugarcane crops, over the years, has focused on crop classification and mapping of planted areas, identification of the development stage through thermal data, discrimination between varieties, production forecasting and the monitoring of health and nutritional status of the crop (Abdel-Rahman; Ahmed, 2008; Rudorff; Aguiar; Silva; Sugawara; Adami; Moreira, 2010;

Adami; Rudorff; Freitas; Aguiar; Sugawara; Mello, 2012). This analysis is usually done with satellite data and it is focused on large areas.

In recent years, research in sugarcane fields has turned to PA using unmanned aerial vehicle (UAVs) and data acquired from orbital sensor systems with refined spatial resolution. Among the applications of remote sensing in PA, with great interest in the management of agricultural crops, is the knowledge about biomass and the forecast of crop productivity. Historically in remote sensing, these estimates have been made using vegetation indices (Kross *et al*. 2015; Todd, Hoffer; Milchunas 1998; Zhou *et al*. 2017).

UAVs and Structure from Motion (SfM) techniques facilitated the construction of canopy elevation and structure models with high spatial resolution, allowing to generate plant height data. Thus, canopy surface models have been successfully used to estimate productivity and biomass in several crops, such as barley (Bendig *et al*. 2015), corn (Zhu *et al*. 2019), and also sugarcane (Sofonia *et al*. 2019), either alone or in conjunction with vegetation indices. Several studies have made canopy height estimates through SfM for different cultures (Paturkar; Gupta; Bailey, 2020; Malambo *et al*., 2018; Souza *et al*., 2017a); however, the direct relationship between canopy height and vegetation indices, with variable spatial resolutions has been little studied.

Thus, this work aims to estimate the height of three different sugarcane varieties, in different development stages, to verify the capability and effectiveness of canopy height estimation models built from UAV data. Additionally, an analysis on the relationship between height at different stages and vegetation indices is made, at different spatial resolutions.

2 MATERIALS AND METHODS

The study area is located in the region of Ribeirão Preto city, NE São Paulo State, Brazil (S21°.18 and W47°.82, the exact location is confidential, under NDA). It is a strong agricultural and agro-industrial pole, with coffee, rubber, peanut, soybean, corn, citrus, sugar cane crops, among others (IEA, 2018). The sugar and alcohol industry is the main

economic activity. It concentrates most of the Brazilian sugarcane production, being the world largest producer of sugar and alcohol (Emplasa, 2016).

The region's climate, according to the Köppen classification, is classified as Aw (Dubreuil *et al*., 2018): tropical with rainy summer and dry winter, average temperatures over 18° C and rainfall rates of approximately 1,500 mm/year (Ayoade, 1996). The predominant soil type is the Red Latosol, known locally as "Terra roxa", due to its great fertility (Rossi, 2017). The terrain is 600 m high, and the highest areas are located at the eastern border, with altitudes above 1000 m. In the western portion are the lowest altitudes, with a minimum of 400 m, characterized by flat terrains with a predominance of plains. In these regions there is a predominance of sugarcane plantation while in the higher parts there is a greater diversity of cultures and preserved areas (Emplasa, 2016),

Table 1 – Characteristics of the area under study

	Area (ha)	Soil type	Date of 1st plantation	Variety	Stage of cust	Date of last harvest
A	23,24	Typic Hapludox	Feb. 20th 2017	CTC9005HB	2nd cut (18 months)	May / 2019
B	16,44	Rhodic Hapludox	Feb. 26th 2017	RB855453	2nd cut (18 months)	April / 2019
C	30,33	Rhodic Hapludox	Dec, 3rd 2014	SP80-3280	4th cut (12 months)	Oct./ 2019

Source: Prepared by the autor

The analysis was carried out in three different plots, due to the availability of auxiliary data and to differences at the sugarcane development. Relevant information about each area is presented in Table 1. Sugarcane is a semi-perennial crop with a growth cycle of 12 or 18 months depending on the variety. It develops in four stages: sprouting, tilling, stalk growth and maturation. The first stage is characterized by the formation and development of leaves, taking 20 to 30 days for sprouting to occur. Tilling is the process of emitting shoots, stems and lateral stems, and occurs around 40 days after planting, lasting up to 120 days. Stalk growth begins after 120 days and can last up to 270 days in a 12-month crop. At this stage 75% of the total dry matter

accumulates. At maturation, there is a reduction in the growth rates of the plants and an increase in the accumulation of sucrose. This phase starts from 270 to 360 days after planting, and can last for up to 6 months (Marafon, 2012).

2.2 UAV data

An aerial survey was carried out on Dec. 19, 2019, using a DJI Phantom 3 UAV, with an RGB camera, resolution of 12.4 Megapixels, image dimensions of 4000 x 3000 pixels and focal length of 20 mm (1/2.3", with f / 2.8 and 94° FOV). No ground control points were collected. The flight height was 100 m above ground, following the planting line, with 80% of lateral and longitudinal overlap. The flight time was around noon, with cloudy sky, and an interval of approximately half an hour between one flight and another.

Figure 1 – Workflow of the main steps to obtain the estimated canopy height of sugarcane in the SE Region of Brazil, using UAV data

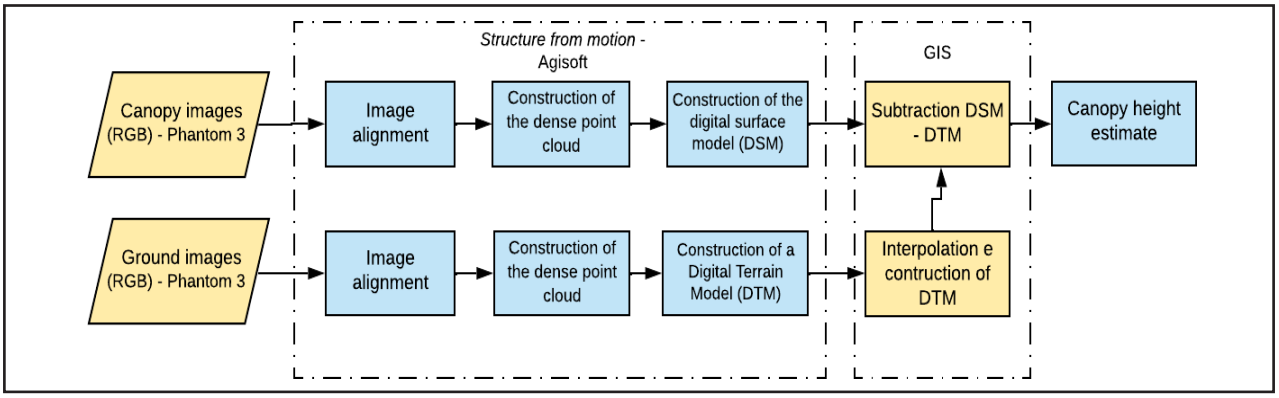

Source: Prepared by the autor

The geo-referencing and processing of UAV images were performed with the Agisoft Metashape software (Agisoft LLC., St. Petersburg, Russia), which allows the generation of elevation and ortho-mosaic models with the SfM algorithm. The photos were aligned considering the highest parameter, followed by the construction of a dense-cloud (no additional corrections were carried out). The parameters considered were ultrahigh for the quality and mild for the depth filter, to preserve the details of the model. Afterwards, the Digital Elevation Model (DEM) and orthomosaics were made, using the software's default settings, considering all points of the dense cloud (Figure 1).

The Digital Terrain Model (DTM) was built by interpolating points with information on ground altitude between the planting lines. These data were obtained from a flight performed on a previous date, when the sugarcane was sufficiently small to visualize the soil. The roads were used as stable ground reference for difference calculation. For areas A and B the DTM was made from images obtained in June 2020, while, for area C, images from Dec. 2020 were used. The height estimation was obtained by subtracting the DEM from the UAV images, and the interpolated DTM (Figure 1). Negative values were standardized to zero.

2.3 Satellite data

To calculate the vegetation indices, multispectral images were acquired from three satellites, with different spatial resolutions: PlanetScope, Sentinel-2 MSI and Landsat 8 OLI. All data were acquired in surface reflectance, and no bandwidth adjustment was performed. The acquisition date was as close as possible to the flight with UAV, on December 17, 26 and 30, respectively. Different spatial resolutions were evaluated to verify its influence on the spatial variance, considering the actual sensors available. NDVI (Rouse *et al*, 1973; Tucker, 1979) and EVI (Justice *et al*., 1998; Huete *et al*., 2002) were used for the correlation with canopy height. The calculation of it was done according to equations 1 and 2, respectively;

$$NDVI = (\rho nir - \rho red) / (\rho nir + \rho red) \quad (1)$$

where ρnir is the reflectance in the near infrared and ρred is the reflectance in the red region.

$$EVI = 2.5 * (\rho nir - \rho red) / (1+ \rho nir + 6 * \rho red - 7.5 * \rho blu) \quad (2)$$

where ρblu is the blue region of the electromagnetic spectrum. Thus, the indices were calculated for each area in three different spatial resolutions, 3, 10 and 30 meters.

2.4 Field information and activities

For each area, an average canopy height was obtained in the field, to compare with the height estimated by the SfM model. To obtain the most representative values of the observed areas, each field collection point was composed of four samples, distributed as vertices in a quadrangular geometry, and the canopy height was measured for each vertex, finally, an average was performed between the heights of the 4 measured points, to obtain the final average height for each area.

Field conditions were also observed, such as the presence of weeds and failures in the planting lines; the height was also assessed visually during imaging with the UAV. Furthermore, meteorological and management data were obtained.

2.5 Data analysis

The estimated average for each area was compared statistically with the average obtained in the field when sugarcane was in the same stage of development. For this purpose, random samples were selected from the models in each area, and those with height equal to zero were removed, and thus, the number of samples was 994, 989 and 421 for areas A, B and C respectively. Initially, a Shapiro-Wilk test (Shapiro; Wilk, 1965) was performed with a significance level (α) of 0.1, to verify the normality of the data. As the p-value results for all areas were less than α ($p < 0.1$), the data did not come from a normal distribution, thus, the Wilcoxon – Mann – Whitney (WMW) test was performed (Neuhäuser, 2011).

To verify whether there is a spatial relationship between canopy height and vegetation indices for the whole area, Pearson's correlation coefficient and the determination coefficient (R^2) between estimated canopy height data and vegetation indices, NDVI and EVI, were calculated. NDVI, EVI and height values were selected and plotted along a transect in each area (indicated with arrows in the Figures 2, 4 and 6), referring to the highest available resolution (3 m). This analysis was performed using software R v.3.6.1.

3 RESULTS

Figure 2 shows the orthomosaic and the estimated canopy height map for area A, with a spatial resolution of 0.10 m. The canopy height ranged from 0 to 5 m, with an average of 3.24 m and Standard Deviation (SD) of 0.55 m, considering only values above 0.50 m. This value was statistically different from the average obtained in the field, of 3.73 m ($p < 0.05$) at 5% significance, in Dec. 2018, based on field samples and comparison of pairs. The lowest heights are located in the central and lower part of the field, while the highest (above 4 m) at the edges and the top, possible related to miss corrections of the model.

Figure 2 – (A) Orthomosaic for study area A processed using SfM in true RGB composition, UAV images obtained in December / 2019. Coordinates are neglected due to NDA. (B) Height map from UAV images for Area A obtained in Dec.2019, 0.10 m spatial resolution, were the border was masked. (C) Section highlighted in the height map and (D) same section as in the orthomosaic. . The arrow indicates the transect where the height samples were taken

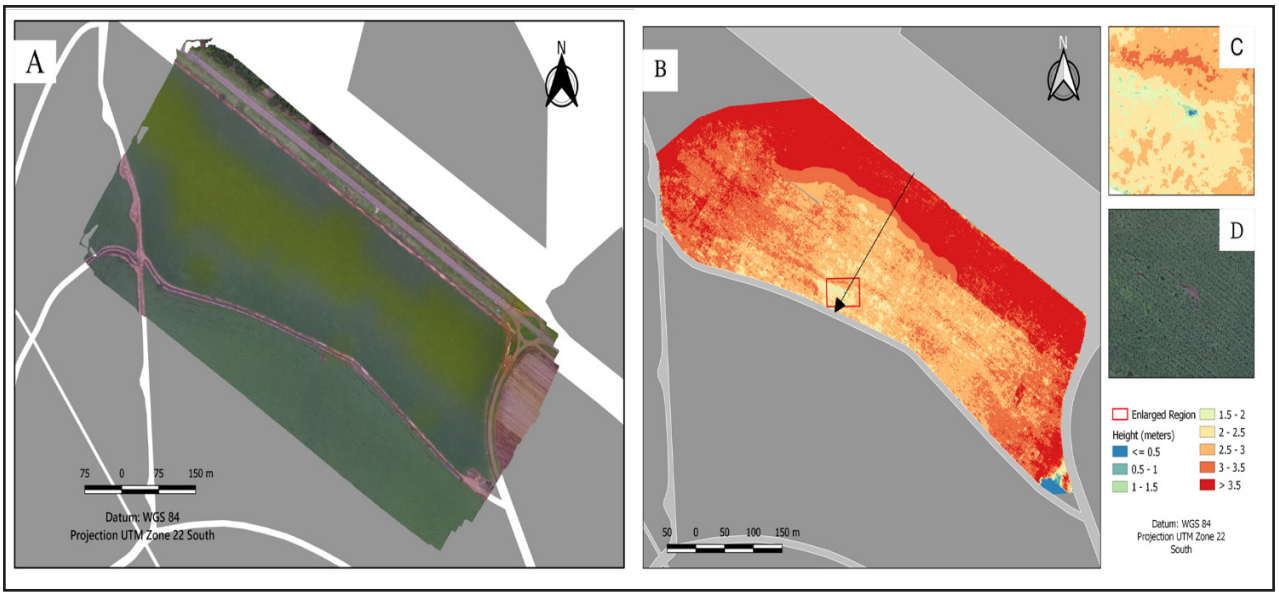

Source: Prepared by the autor

The NDVI values from images of the three satellites, ranged from 0.37 to 0.79 (PlanetScope), from 0.12 to 0.89 (Sentinel-2 MSI) and from 0.17 to 0.85 (Landsat 8 OLI).

Regarding the range of EVI values, as follows: 0.25 to 0.65 (PlanetScope), 0.05 to 0.70 (Sentinel-2) and 0.01 to 0.63 (Landsat 8) (Figure 3). Both indices showed a large spatial variation, which is smaller at 3 m spatial resolution, possible due to its largest bandwidth (early generation of PlanetScope cubsats). No in-depth analysis of the bandwidth was performed; however, its largest bandwidth increases its covariation.

Figure 3 – Per-field variation of vegetation indices (NDVI and EVI) for area A, according to the spatial resolution of orbital data. At the base of the figure a natural color composition of each image is presented

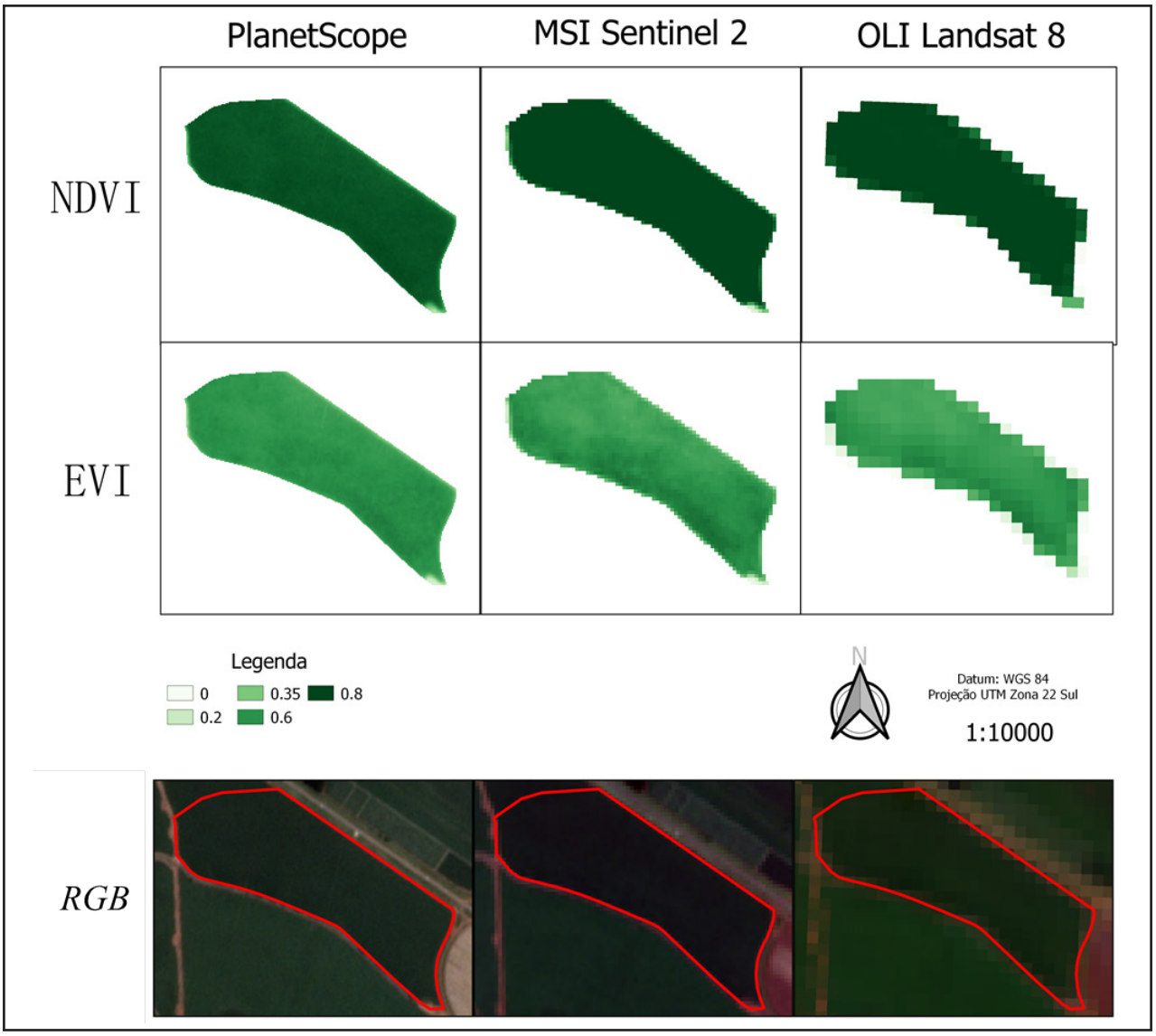

Source: Prepared by the autor

At figure 3, the lowest IV values are found mainly in the areas at the edge of the field, which probably is due to a stronger mixture with bare soil pixels in this section.

At Table 2, the indices did not correlate with height, at any spatial resolution, on both Pearson's and the Determination coefficients.

Figure 4 – (A) Orthomosaic of study area B processed with SfM in true RGB composition, UAV images December / 2019. Coordinates are neglected due to NDA. (B) Height map of UAV images, Area B, Dec. 2019, 0.10 m spatial resolution, where the border was masked. (C) Enlarged section in height map, (D) Orthomosaic of the same section. Different scales are adopted in the figure. The arrow indicates the transect where the height samples were taken

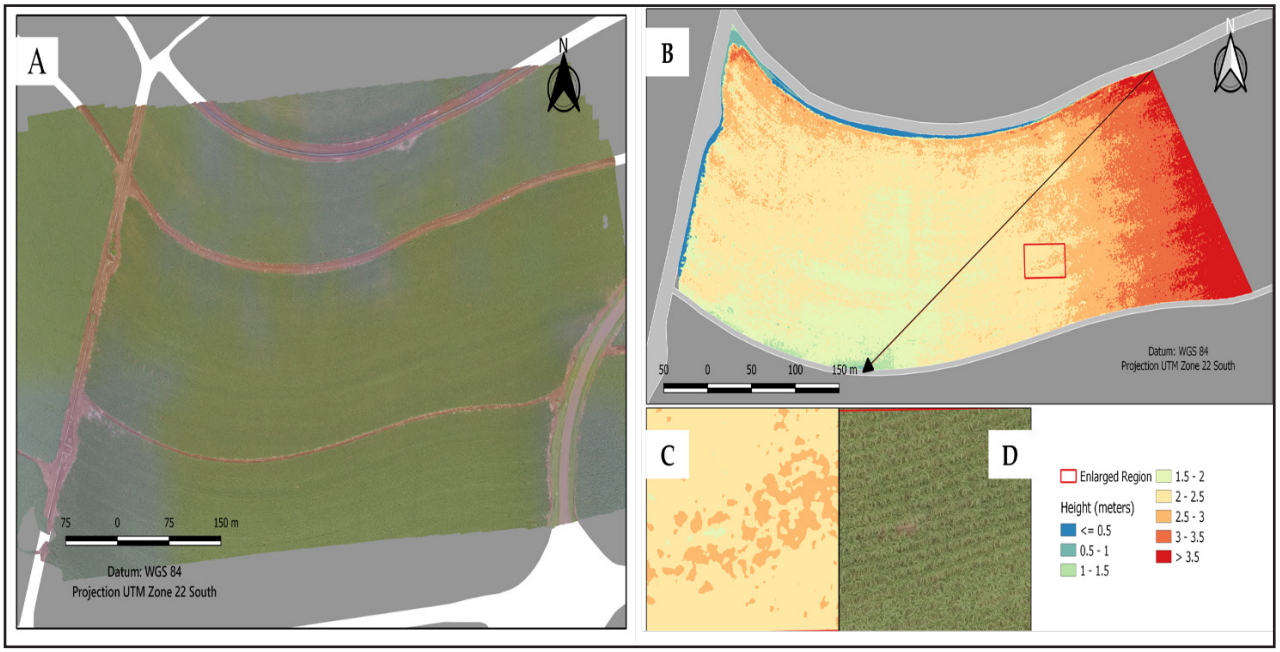

Source: Prepared by the autor

Figure 4 shows the orthomosaic and the height map estimated for area B, with a spatial resolution of 0.10 m. For area B the estimated height values varied from approximately 0 to 4 m, with an average of 2.46 m and a SD of 0.57 m, considering only values above 0.50 m. The lowest heights are located in the central portion of the field and the highest in the eastern section. At this point it is important to highlight the potential implications of ground control points (GCPs) absence for an effective access of the terrain model. Due to the lack of height data measured in the field, referring to the same stage of the sugarcane development, a visual height estimate was made at the date of drone imaging, which is approximately 2.30 m (absence of field

measurements). The result of the WMW analysis indicates that the average obtained during field measurements and estimated, are statistically different ($p < 0.05$) at 5% significance, although their values are close.

Figure 5 – Per-field variation of vegetation indices (NDVI and EVI) for area B, according to the spatial resolution of orbital data. The natural color composition of each image is at the bottom of the figure

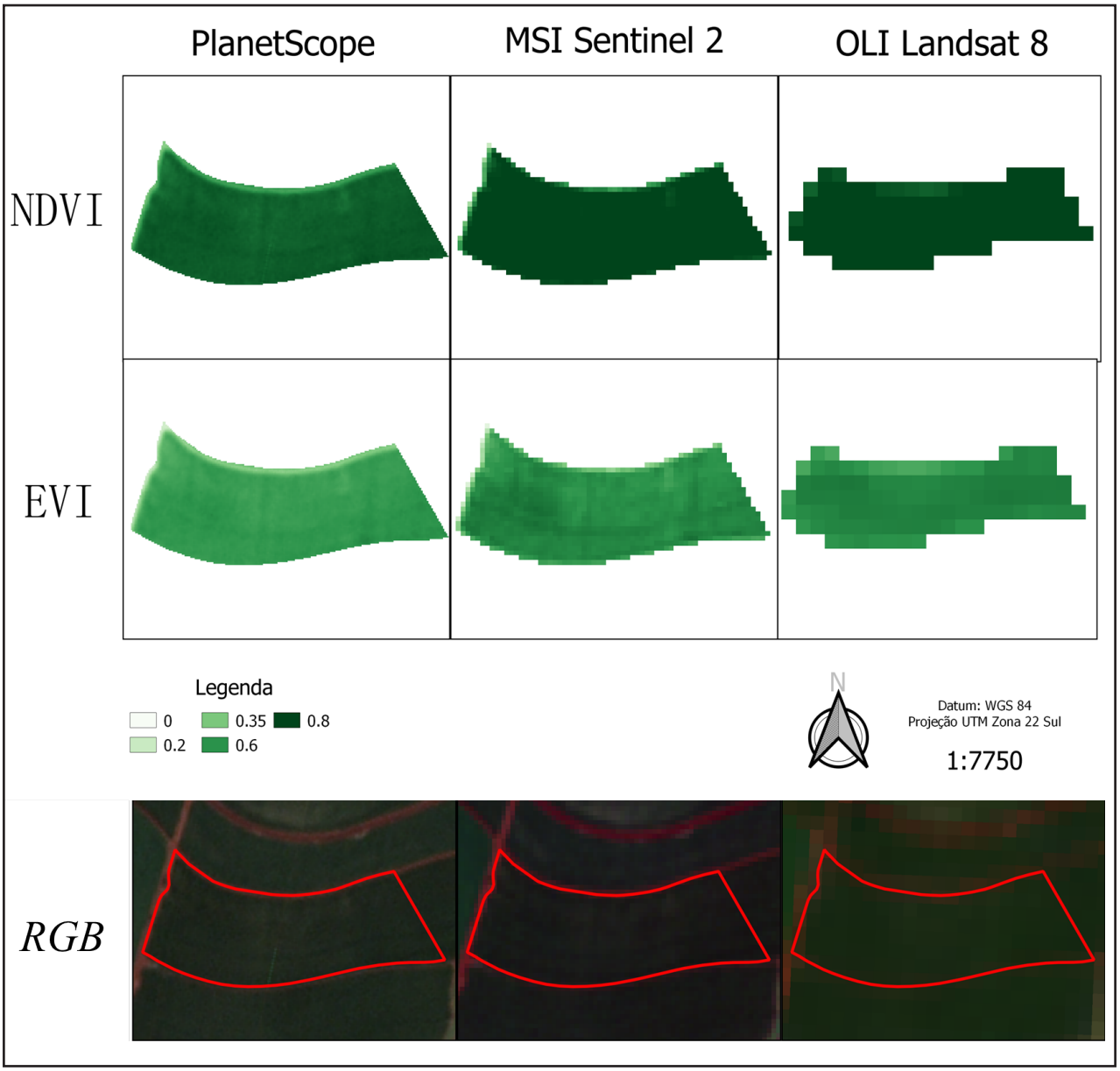

Source: Prepared by the autor

For the three satellite images used, the NDVI values ranged as follows: 0.32 to 0.78 (PlanetScope), 0.21 to 0.89 (Sentinel-2) and 0.72 to 0.85 (Landsat 8). The EVI varied

from 0.17 to 0.64 (PlanetScope), 0.09 to 0.70 (Sentinel-2) and 0.50 to 0.67 (Landsat 8) (Figure 5). Both indices showed great spatial variation in resolutions of 3 and 10 m, and less variation at 30 m. This occurs because larger pixels end up homogenizing large areas, while smaller pixels present a greater variety of details. Again, the lowest values of VIs are located mainly on the edges of the field. The results of the spatial correlation analysis are shown in Table 2. The NDVI showed higher correlation values with canopy height than the EVI in all spatial resolutions. Nevertheless, these results do not indicate any type of correlation between the variables analyzed.

Figure 6 – (A) Ortho-mosaic, study area C processed with SfM, true RGB composition, UAV images from Dec. / 2019. Coordinates are neglected due to NDA. (B) Height map from UAV images for Area C, Dec. 2019, 0.10 m spatial resolution, where the border was masked, (C) Enlarged section of height map, (D) same area in ortho-mosaic. . The arrow indicates the transect where the height samples were taken

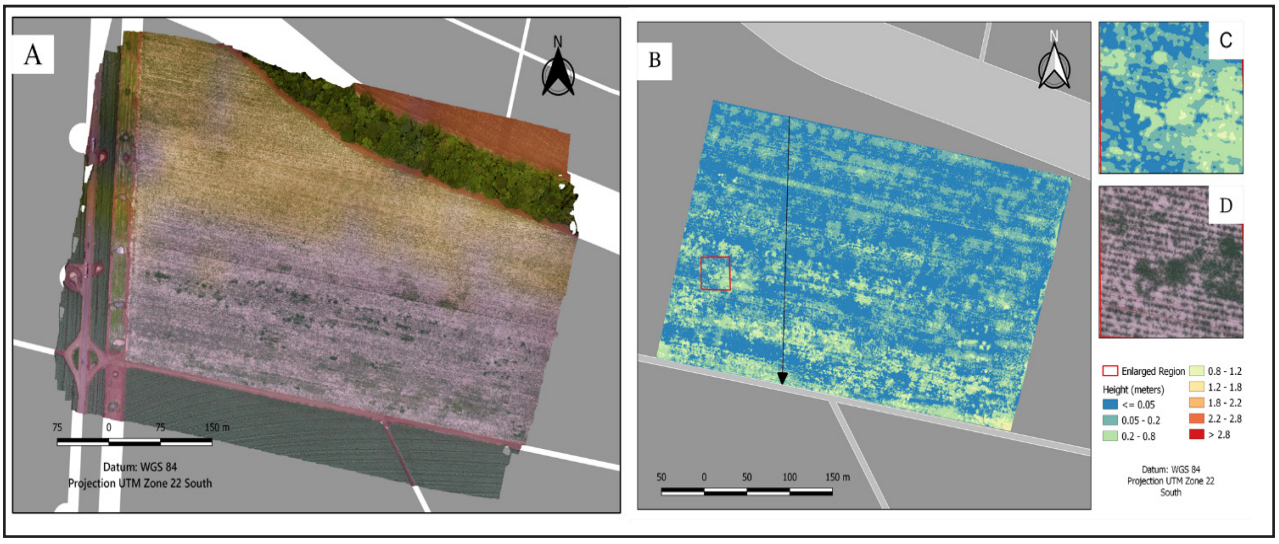

Source: Prepared by the autor

Figure 6 shows the ortho-mosaic and the estimated canopy height map for area C, with a spatial resolution of 0.10 m. The height values estimated for area C have amplitude of 0 to 1.4 m, with an average of 0.20 m and a SD of 0.18 m, considering only values above 0.05 m. The average obtained in the field, referring to the same stage of development, was 0.33 m, showing a significant difference from the estimated average

(p <0.05) according to the WMW test using multiple pairs of points. The height values were slightly above those in the lower portion of the field, and there are flaws in the planting lines, also observed in the field.

Figure 7 – Per-field variation of vegetation indices (NDVI and EVI) for area C, according to the spatial resolution of orbital data. The natural color composition of each image is at the bottom of the figure

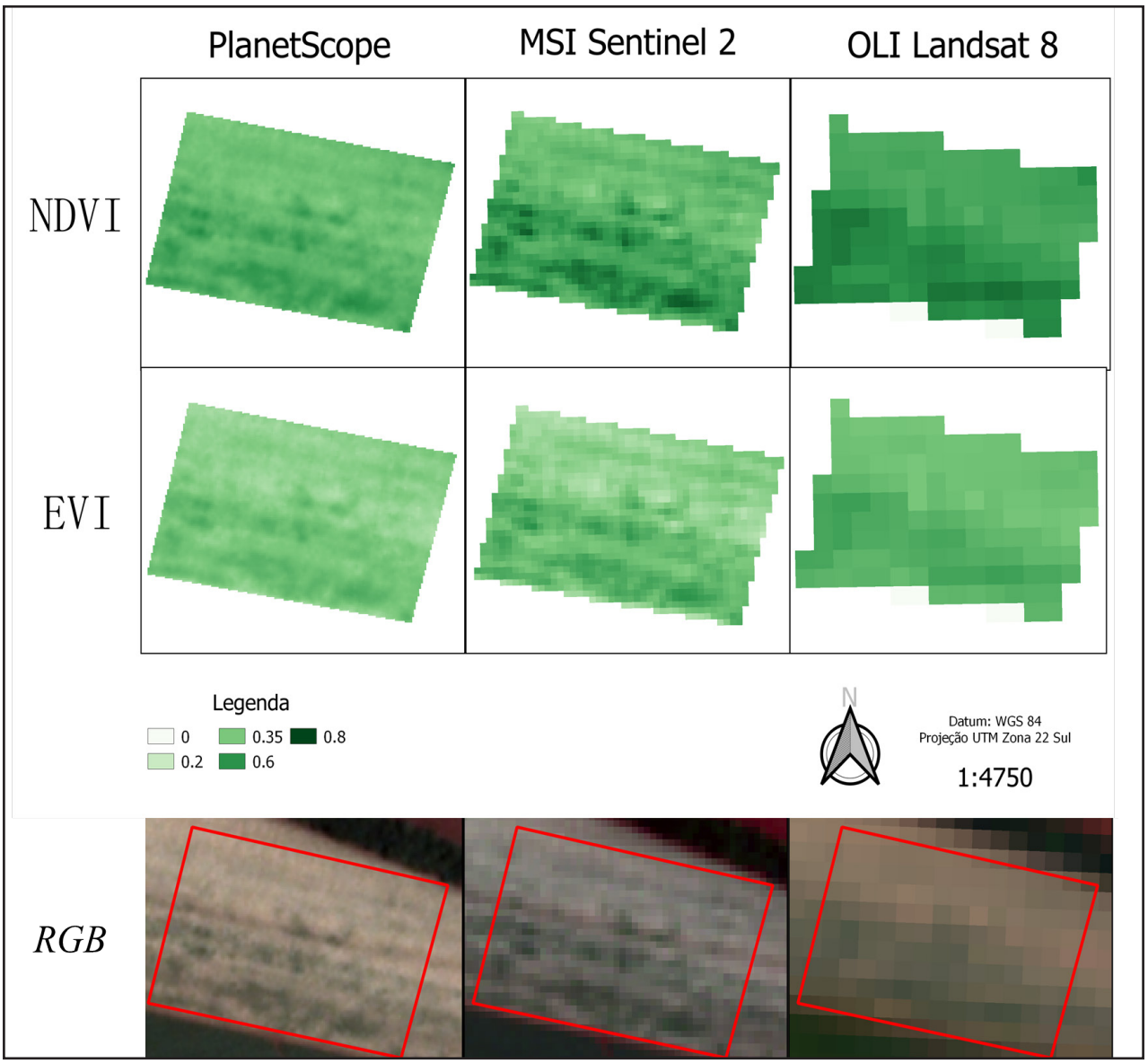

Source: Prepared by the autor

For Area C, the NDVI values ranged from 0.34 to 0.58 (PlanetScope), 0.29 to 0.75 (Sentinel-2) and 0.37 to 0.66 (Landsat 8). The EVI varied from 0.23 to 0.45 (PlanetScope), 0.21 to 0.60 (Sentinel-2) and 0.26 to 0.53 (Landsat 8) (Figure 7). The EVI index showed

lower values than the NDVI, similarly to the other areas analyzed, which can be due to the higher saturation of this index, as compared to EVI. In this area, the height did also not correlate with the indices at any spatial resolution (Table 2). However, at 30 m spatial resolution, the correlation values, for both Pearson and R^2, were lower. Here probably there is a greater mixture of soil and vegetation pixels, while at higher resolutions there is a tendency for pure pixels. At the maps of Figure 7 one verifies that in the lower portion of the plot, sugarcane is more robust, also observed on the Height Map.

Table 2 – Pearson and R^2 correlation values for Areas A, B and C

		3 m		10 m		30 m	
		Person	**R^2**	**Person**	**R^2**	**Person**	**R^2**
Area A	*NDVI*	*0.0707*	*0.0109*	*0.0960*	*0.0133*	*0.0996*	*0.099*
	EVI	*-0.0402*	*0.0352*	*-0.1255*	*0.0869*	*-0.1032*	*0.0106*
Area B	*NDVI*	*0.2626*	*0.069*	*0.2041*	*0.0417*	*0.4184*	*0.175*
	EVI	*0.2172*	*0.0472*	*0.1285*	*0.0135*	*0.3287*	*0.1155*
Area C	*NDVI*	*0.3610*	*0.1303*	*0.3475*	*0.1207*	*0.1578*	*0.0249*
	EVI	*0.3303*	*0.1091*	*0.3189*	*0.1017*	*0.1366*	*0.0187*

Source: Prepared by the autor

4 DICUSSION

The height models showed satisfactory results, with average values close to those obtained in the field measurements, despite not being statistically significant. Except for area B, where the average estimated by the model was higher than that one estimated in the field measurements, the models have a tendency to underestimate the height, also found out by other authors (Willkomm; Bolten; Bareth, 2016; Aasen *et al*., 2015). Additionally, the averages obtained with SfM are continuous and encompass all the internal micro-variability of the canopy, while for field measurements a homogeneous area was selected, seeking to be as representative as possible, but it did not encompass all its variability. Unfortunately, no densification of field samples could

be conducted to include the spatial variability within the plot. Such internal variability can be a proxy to delineate management zones (Breunig *et al*., 2020b). Thus, for the direct comparison of averages, a lower average is expected for data derived from UAVs. However, the significant difference between the averages does not disqualify any of the products obtained. Using Height models, it was also possible to identify flaws in the planting lines for all areas, as shown in the enlargements of figures 2, 4 and 6. The model showed more flaws in the smallest stage of development of sugarcane (area C), and some sections with very small plants were not identified, due to the omission of the Height model.

Souza *et al*. (2017b) when estimating the height of sugarcane with high resolution images and different acquisition geometries (N - S and E - W) found that the shadow affects the quality of the model obtained, and that an approach combining the two different flight planes generated models with less errors, softening the shadow effect on the images. Bendig *et al*. (2013) concluded that different image acquisition geometries can lead to better results, especially when there are large height differences. This procedure however requires a longer acquisition time, thus, imaging at nadir close to noon could mitigate this effect without the need for an extra flight.

The use of ground control points (GCPs) could provide significant improvements in the accuracy of the model, as evidenced by Ruiz *et al*. (2013) and Turner, Lucieer and Watson (2012), who concluded that geo-referencing done exclusively by GPS onboard an UAV, increases the errors in the SfM algorithms. In spite of that, through the models created in our study, it was possible to identify flaws in the planting lines at the first stage of sugarcane growth (Area C), in addition to sections of lower development within the plot, as observed in areas A and B.

Both vegetation indices showed large spatial variation, mainly in areas A and B. According to Bégué *et al*. (2010) the variations of vegetation indices, specifically the NDVI, are mainly caused by phenological factors and climatic conditions during data acquisition. These authors also mention management practices as a determining factor for spatial variability in sugarcane fields. The NDVI showed a higher saturation in

relation to EVI, as shown in Figures 3, 4 and 7. Due to its lower saturation and greater sensibility to structural parameters, small variations are more evident in EVI at all resolutions. It is different for NDVI, where, at 10 and 30 m spatial resolution, the field seems quite homogeneous, except for area C, where these variations are visible, due to a larger amount of soil and a lower spectral response of vegetation.

Figure 8 – VIs of sugarcane vs. estimated height for the transects in each area: (a) Area A, (b) Area B, (c) Area C. Transect is indicated by an arrow over the figures 2, 4 and 6

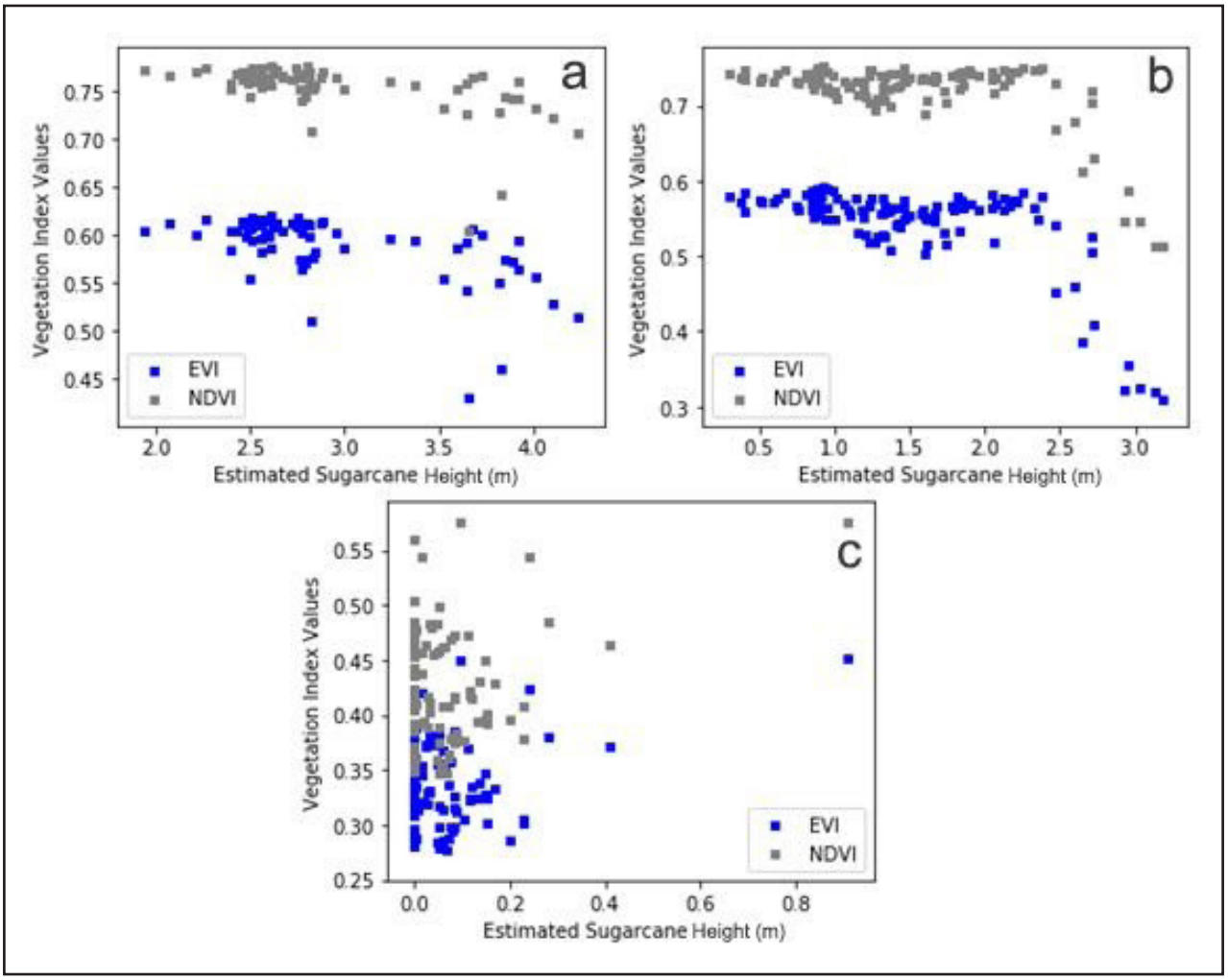

Source: Prepared by the autor

For the three areas, the results of spatial correlation analysis did not indicate a direct relationship between canopy height and vegetation indices. Figure 8 confirms this, where the index values are independent from the observed heights. The transects were selected to show specific regions and highlight possible differences, instead to

the use of all data per-plot. However, the NDVI showed higher correlation values with height than EVI in all spatial resolutions, excluding area A, where EVI presented higher R^2 values. Nevertheless, since it represents a single period and little variation in height was observed, the data variability is too small to obtain more significant correlations between the VIs and the Height data. The rapid drop of the vegetation indices in Figure 8A and Figure 8B seems related to a border effect or possible canopy height model errors due to the absence of GCPs.

Comparing the results between spatial resolutions, no relevant differences were observed, indicating that resolution was not a limiting factor in this case (Breunig *et al*., 2020b). It should be emphasized that the VIs analyzed have different formulation principles. NDVI is an index related especially to pigments (chlorophylls) and EVI is strongly related to structural parameters of the canopy and has a strong correlation with the near infrared band (Leblon; Granberg; Charland, 1996; Huete *et al*., 2002; Galvão *et al*., 2018).

Payero *et al*. (2004) compared the ability of 11 vegetation indices to estimate the height of alfalfa and grass plants. They found a good logistical relationship between the indices and the height for alfalfa ($R^2 > 0.90$). The NDVI, IPVI and TVI indices however became insensitive to plant growth when they exceeded 0.40 m height. For grass, the indices showed a lower performance in height estimation, and only the RATIO, TVI, NDVI and IPVI indices presented a good linear relationship ($R^2 \approx 0.76$). Thus, the responses of these indices vary according to the characteristics of vegetation and of its phenological stage. For this task, a temporal analysis is of fundamental importance, to verify its behavior at different stages of the culture development, besides the evaluation of other indices.

In spite of that, both the height and the vegetation indices can be related to productivity and biomass. Bendig *et al.* (2015) found that the combination of vegetation indices and height information generated an improved model for estimating biomass when compared to a model using only one variable. Yu *et al*. (2020), by incorporating height measures in a production estimate model for sugarcane, observed an

improvement of the results obtained. They concluded that the measures taken in the last development stage produced more significant results, and so it is unnecessary to sample the entire development period. Therefore, even without presenting a direct relationship, these variables can complement each other in the analysis of other vegetation properties.

Furthermore, the analysis made with UAV images, highlighted the importance of the spatial continuity, showing the micro-variability within the field, and allowing a more precise and detailed evaluation than by traditional field inspection. This information is essential for decision making and for increasing production efficiency, because it reduces errors due to possible poor representativeness of samples in the field.

5 CONCLUSION

The results obtained in this work demonstrates the potential of using UAVs to estimate the height of plantations, such as sugarcane. Using the plantation surface model, it was possible to spatially determine the different growth patterns, and thus, allowing direct management practices to the specific needs of each portion from the stand. The models tended to underestimate the heights, which could be improved with the use of GCPs or UAVs with post-processed positioning (PPK), as well as with the reduction of the shadow effect.

The correlation analysis did not indicate any direct relationship between vegetation indexes and height. Nevertheless, a temporal analysis is necessary to present more consistent conclusions. Such an analysis will be carried out in future works. The spatial resolution was not a limiting factor. We recommend however to consider higher resolutions in the early stages of the plantation growth, when there is still a considerable portion of bare soil, which could increase errors due to mixed pixels. These variables are important to estimate other vegetation parameters, such as biomass and productivity, as advised by several authors.

ACKNOWLEDGEMENTS

We acknowledge the National Council for Scientific and Technological Development - CNPq (Process Nr. 309030/2017-0, 130575/2019-4, and 305084/2020-8) which funded this Project. Planet Labs R&D Engineering Sync program (NDA - LGSR/UFSM-FW) delivered the PlanetScope images.

REFERENCES

AASEN, H., et al Generating 3D hyperspectral information with lightweight UAV snapshot cameras for vegetation monitoring: From camera calibration to quality assurance. **ISPRS Journal of Photogrammetry and Remote Sensing**, v. 108, p. 245-259. Oct. 2015.

ABDEL-RAHMAN, E. M.; AHMED, F. B. The application of remote sensing techniques to sugarcane (Saccharum spp. hybrid) production: a review of the literature. **International Journal of Remote Sensing**, v. 29, n. 13, p. 3753-3767, 14 jun. 2008.

ADAMI, M. et al. Remote Sensing Time Series to Evaluate Direct Land Use Change of Recent Expanded Sugarcane Crop in Brazil. **Sustainability**, v. 4, n. 4, p. 574-585, 2 apr. 2012.

AYOADE, J. O. **Introdução à climatologia para os trópicos**. 4. ed. Rio de Janeiro: Bertrand Brasil, 1996.

BÉGUÉ, A. et al. Spatio-temporal variability of sugarcane fields and recommendations for yield forecast using NDVI. **International Journal of Remote Sensing,** v. 31, n. 20, p. 5391-5407, oct. 2010.

BENDIG, J.; BOLTEN, A.; BARETH, G. UAV-based Imaging for Multi-Temporal, very high Resolution Crop Surface Models to monitor Crop Growth Variability. **Photogrammetrie - Fernerkundung - Geoinformation**, v. 2013, n. 6, p.551-562, dec. 2013.

BENDIG, J. et al. Combining UAV-based plant height from crop surface models, visible, and near infrared vegetation indices for biomass monitoring in barley. **International Journal Of Applied Earth Observation And Geoinformation.** v. 39, p.79-87, Jul. 2015.

BIAN, J. et al. Simplified Evaluation of Cotton Water Stress Using High Resolution Unmanned Aerial Vehicle Thermal Imagery. **Remote Sensing.** v. 11, n. 3, p. 267-284, Jan. 2019.

BREUNIG, F. M. et al. Delineation of management zones in agricultural fields using cover–crop biomass estimates from PlanetScope data. **International Journal Of Applied Earth Observation And Geoinformation.** v. 85, p.102004-102019, mar. 2020a.

BREUNIG, F. M., et al. Assessing the Effect of Spatial Resolution on the Delineation of Management Zones for Smallholder Farming in Southern Brazil. **Remote Sensing Applications**: Society and Environment. , v. 19, p. 100325, Aug. 2020b.

CHU, T. et al. Assessing Lodging Severity over an Experimental Maize (*Zea mays L*.) Field Using UAS Images. **Remote Sensing***,* v. 9, n. 9, p.923-947, Sept. 2017.

CONAB - Companhia Nacional De Abastecimento. **Acompanhamento da safra brasileira de cana-de-açúcar- Safra 2019/20.** 4. ed. Brasília: Estúdio Nous, 2020. Available at: https://www.conab.gov.br/. Access: Oct. 17th 2020.

DAMIAN, J. M. et al. Monitoring variability in cash-crop yield caused by previous cultivation of a cover crop under a no-tillage system. Computers And Electronics In Agriculture, v. 142, p. 607-621,Nov. 2017.

DAMIAN, J. M. et al. Applying the NDVI from satellite images in delimiting management zones for annual crops. **Scientia Agricola**, v. 77, n. 1, p. 1-11, 2020.

DUBREUIL, V., et al. The types of annual climates in Brazil: an application of the classification of Köppen from 1961 to 2015. **Confins**, n. 37, p.1-20, Jan. 2018. *In Portuguese.*

ELARAB, M. et al. Estimating chlorophyll with thermal and broadband multispectral high-resolution imagery from an unmanned aerial system using relevance vector machines for precision agriculture. **International Journal Of Applied Earth Observation And Geoinformation**, v. 43, p.32-42, Apr. 2015.

EMPLASA. **Região Metropolitana de Ribeirão Preto:** estudos técnicos. 2016. Avaliable at: emplasa.sp.gov.br/Cms_Data/Contents/Emplasa/Media/publicacoes/RMRP_estudos_tecnicos.pdf. Access: Nov. 30th 2020.

GALVÃO, L. S. et al. Crop Type Discrimination Using Hyperspectral Data: Advances and Perspectives, in **Biophysical and Biochemical Characterization and Plant Species Studies**, ed. by Alfredo Huete Prasad S. Thenkabail, John G. Lyon, 2nd ed. (Boca Raton, FL: CRC Press, 2018), p. 183–211. <https://doi.org/10.1201/9780429431180>

GRÜNER, E.; ASTOR, T.; WACHENDORF, M. Biomass Prediction of Heterogeneous Temperate Grasslands Using an SfM Approach Based on UAV Imaging, **Agronomy***,* v. 9, n. 2, p.54-70, Jan. 2019.

HOFFMANN, H. et al. Crop water stress maps for an entire growing season from visible and thermal UAV imagery, **Biogeosciences***,* v. 13, n. 24, p.6545-6563, dec. 2016.

HUETE, A.et al. Overview of the radiometric and biophysical performance of the MODIS vegetation indices. **Remote Sensing Of Environment**, v. 83, n. 1-2, p. 195-213, Mar. 2002.

HUNT E. R.; DAUGHTRY, C. S. T. What good are unmanned aircraft systems for agricultural remote sensing and precision agriculture? **International Journal Of Remote Sensing***,* v. 39, n. 15-16, p.5345-5376, Dec. 2017.

IEA - INSTITUTO DE ECONOMIA AGRÍCOLA. **Estatísticas da Produção Agrícola:** Período de 2017 à 2018. 2018. Available at: http://ciagri.iea.sp.gov.br/nia1/subjetiva.aspx?cod_sis=1&idioma=1 Access: Jan.23rd. 2020.

IVUSHKIN, K. et al. UAV based soil salinity assessment of cropland, **Geoderma**, v. 338, p.502-512, Mar. 2019.

JUSTICE, C. O. et al. The Moderate Resolution Imaging Spectroradiometer (MODIS): land remote sensing for global change research. **IEEE Transactions on Geoscience and Remote Sensing**, v.36, n.4, p.1228-1249, Jul. 1998.

KROSS, A., et al. Assessment of RapidEye vegetation indices for estimation of leaf area index and biomass in corn and soybean crops, **International Journal of Applied Earth Observation and Geoinformation,** v. 34, p. 235-248, Feb. 2015.

LEBLON, B.; GRANBERG, H.; CHARLAND, S.D. Shadowing effects on SPOT-HRV and high spectral resolution reflectance in Christmas tree plantations. **International Journal Of Remote Sensing,** v. 17, n. 2, p. 277-289, Jan. 1996.

LIU, T. et al. Estimates of rice lodging using indices derived from UAV visible and thermal infrared images. **Agricultural And Forest Meteorology**, v. 252, p.144-154, Jan. 2018.

LUNA, I.; LOBO, A. Mapping Crop Planting Quality in Sugarcane from UAV Imagery: a pilot study in Nicaragua. **Remote Sensing**, v. 8, n. 6, p. 500-518, Jun. 2016.

MALAMBO, L. et al. Multitemporal field-based plant height estimation using 3D point clouds generated from small unmanned aerial systems high-resolution imagery, **International Journal of Applied Earth Observation and Geoinformation,** v. 64, Feb. 2018.

MARAFON, A. C. **Análise Quantitativa de Crescimento em Cana de- açúcar: uma introdução ao procedimento prático**. Aracaju: Embrapa Tabuleiros Costeiros, 29 p. (Documentos / Embrapa Tabuleiros Costeiros, ISSN 1678-1953; 168), 2012. Available at: http://www.cpatc.embrapa.br/publicacoes_2012/doc_168.pdf. Access: Jul.15th. 2020

MULLA, D. J. Twenty five years of remote sensing in precision agriculture: Key advances and remaining knowledge gaps, **Biosystems Engineering**, v. 114, p. 358-371, Apr. 2013.

NEUHÄUSER M. Wilcoxon–Mann–Whitney Test. In: LOVRIC, M. (eds) **International Encyclopedia of Statistical Science.** Berlin, Heidelberg: Springer, 2011.

PATURKAR, A.; GUPTA, G.S.; BAILEY, D. Non-destructive and cost-effective 3D plant growth monitoring system in outdoor conditions. **Multimedia Tools And Applications**. v. 79, n. 47-48, p. 34955-34971,Apr. 2020.

PAYERO, J. O.; NEALE, C. M. U.; WRIGHT, J. L. Comparison Of Eleven Vegetation Indices For Estimating Plant Height Of Alfalfa And Grass, **Applied Engineering in Agriculture**, v. 20, p. 385-393, 2004.

QUEBRAJO, L. et al. Linking thermal imaging and soil remote sensing to enhance irrigation management of sugar beet, **Biosystems Engineering**, v. 165, p.77-87, Jan. 2018.

ROSSI, M. **Mapa pedológico do Estado de São Paulo**: revisado e ampliado. São Paulo: Instituto Florestal, v.1. 118 p., 2017. (Inclui Mapas)

ROUSE, J. Wet al. Monitoring vegetation systems in the great plains with ERTS. In: Earth Resources Technology Satellite-1 Symposium, 3., Washington, D.C., 1973. **Proceedings**. Washington, D.C.: NASA. Goddard Space Flight Center, 1973. v.1, p.309-317. (NASA SP-351).

RUDORFF, B. F. T., et al. Studies on the Rapid Expansion of Sugarcane for Ethanol Production in São Paulo State (Brazil) Using Landsat Data. **Remote Sensing**, v. 2, n. 4, p. 1057-1076, Apr. 2010.

RUIZ, J.J et al. Evaluating the accuracy of DEM generation algorithms from UAV imagery. **International Archives of the Photogrammetry**, Remote Sensing and Spatial Information Sciences. 2013, 40, 333–337.

SANCHES, G. M. et al. The potential for RGB images obtained using Unmanned Aerial Vehicle to assess and predict yield in sugarcane fields, **International Journal Of Remote Sensing**, v. 39, n. 15-16, p.5402-5414, Mar. 2018.

SANTESTEBAN, L. G. et al. High-resolution UAV-based thermal imaging to estimate the instantaneous and seasonal variability of plant water status within a vineyard, **Agricultural Water Management**, v. 183, p.49-59, Mar. 2017.

SHAPIRO, S. S.; WILK, M. B. An analysis of variance test for normality (complete samples). **Biometrika**, *52* (3–4), p. 591–611, 1965.

SOFONIA, J. et al. Monitoring sugarcane growth response to varying nitrogen application rates: A comparison of UAV SLAM LiDAR and photogrammetry. **International Journal Of Applied Earth Observation And Geoinformation**, v. 82, p.101878-101893, Oct. 2019.

SOUZA, C. H. W. et al. Mapping skips in sugarcane fields using object-based analysis of unmanned aerial vehicle (UAV) images. **Computers and Electronics in Agriculture**, v. 143, p.49-56, Dec. 2017a.

SOUZA, C. H. W.de et al. Height estimation of sugarcane using an unmanned aerial system (UAS) based on structure from motion (SfM) point clouds. **International Journal of Remote Sensing**, v. 38, n. 8-10, p.2218-2230, Jan. 2017b.

TODD, S. W.; HOFFER R. M.; MILCHUNAS D. G. Biomass estimation on grazed and un-grazed rangelands using spectral indices, **International Journal of Remote Sensing**, p. 427-438, Jan. 1998.

TUCKER, C. J. Red and Photographic Infrared Linear Combinations for Monitoring Vegetation. **Remote Sensing Of Environment,** n. 8, p. 127-150, 1979.

TURNER, D.; LUCIEER, A.; WATSON, C. An automated technique for generating geo-rectified mosaics from Ultra-high resolution Unmanned Aerial Vehicle (UAV) imagery, based on Structure from Motion (SfM) point clouds. **Remote Sensing**, v. 4, 1392–1410, 2012.

WILLKOMM, M.; BOLTEN, A.; BARETH, G. Non-destructive monitoring of rice by hyperspectral in-field spectrometry and UAV-based remote sensing: Case study of field-grown rice in north Rhine-Westphalia, Germany, **ISPRS Int. Arch. Photogramm**. Remote Sens. Spat. Inf. Sci. XLI-B1, 1071–1077, 2016.

YU, D. et al. Improvement of sugarcane yield estimation by assimilating UAV-derived plant height observations. **European Journal of Agronomy**. V. 121(126159), p. 1-16, 2020.

ZHANG, N.; WANG, M.; WANG, N. Precision agriculture—a worldwide overview, **Computers And Electronics In Agriculture***,* v. 36, n. 2-3, p.113-132, Nov. 2002.

ZHOU, X et al. Predicting grain yield in rice using multi-temporal vegetation indices from UAV-based multispectral and digital imagery, **ISPRS Journal Of Photogrammetry And Remote Sensing,** v. 130, p.246-255, Aug. 2017.

ZHU, W. et al. Estimating Maize Above-Ground Biomass Using 3D Point Clouds of Multi-Source Unmanned Aerial Vehicle Data at Multi-Spatial Scales. **Remote Sensing***,* v. 11, n. 22, p.2678-2700, Nov. 2019.

Contribuição de autoria

1 – Gabriela Zoli Simões

Engenheira Ambiental pela Universidae Tecnológica Federal do Paraná
https://orcid.org/0000-0002-3089-1970• gabriela.simoes@inpe.br
Contribuição: Escrita – primeira redação, Escrita – revisão e edição; Curadoria de dados, Conceituação

2 – Hermann Johann Heinrich Kux

Geógrafo formanda pela Universidade de São Paulo, com doutorado em Geologia pela Universidade Freiburg na Alemanha
https://orcid.org/0000-0002-5502-0688 • hermann.kux@inpe.br
Contribuição: Escrita – revisão e edição, Conceituação, Supervisão

3 – Fábio Marcelo Breuning

Geógrafo formando pela Universidade Federal de Santa Maria, com mestrado e doutorado em Sensoriamento Remoto pelo Instituto de Pesquisas Espaciais
https://orcid.org/0000-0002-0405-9603 • breunig@ufsm.br
Contribuição: Escrita – revisão e edição, Conceituação, Supervisão

4 – Luiz Henrique Pereira

Geógrafo formando pela UNESP, com mestrado e doutorado em Análise Ambiental e Geoprocessamento pelo Programa de Pós-Graduação em Geografia
link do Orcid • luiz.pereira@idgeo.com.br
Contribuição: Escrita – revisão e edição, Conceituação, Supervisão

Como citar este artigo

SIMÕES, G.Z.; KUX, H.J.H.; BREUNING, F.M.; PEREIRA, L.H.; Canopy height estimation of sugarcane varieties using an unmanned aerial vehicle (UAV) and integration to satellite images. **Geografia Ensino & Pesquisa**, Santa Maria, v. 27, e65070, p. 1-25, 2023. DOI 10.5902/2236499465070. Disponível em: https://doi.org/10.5902/2236499465070. Acesso em: dia mês abreviado. ano.